

level (Table IV). Thus the upper limit to the mean lifetime of this level (Table III) is consistent with expectations for this isotopic-spin-allowed dipole transition.

ACKNOWLEDGMENTS

We would like to thank Professor A. Gallmann and Dr. R. M. Freeman for helpful discussions and communications.

$^{14}\text{N}(^3\text{He},t)^{14}\text{O}$ Reaction and Excited Isospin Triads in Mass 14*

GORDON C. BALL AND JOSEPH CERNY

Department of Chemistry and Lawrence Radiation Laboratory, University of California, Berkeley, California

(Received 3 November 1966)

The $^{14}\text{N}(^3\text{He},t)^{14}\text{O}$ reaction has been investigated at a ^3He energy of 44.6 MeV. New levels were observed in ^{14}O up to an excitation energy of 18 MeV. An investigation of the $(^3\text{He},t)$ reaction on several other nuclei in the $1p$ shell, notably ^{14}C and ^{15}N , revealed that the shapes and relative magnitudes of the angular distributions arising from single-particle transitions appear to fall into groups which are characterized by the specific shell-model transition involved. Utilizing this effect and other data, it was possible to make most probable spin and parity assignments of $(1-)$, $(0+)$, $(3-)$, $2+$, $(2-)$, and $2+$ for the levels observed in ^{14}O at 5.17, 5.91, 6.28, 6.60, 6.79, and 7.78 MeV, respectively. A correspondence can now be established for six excited $T=1$ levels in all three members of the mass-14 triad.

I. INTRODUCTION

VARIOUS theoretical treatments have been able to predict with reasonable accuracy the Coulomb energy differences observed in ground isobaric multiplets of $T \leq 1$ nuclei, particularly in the $1p$ shell.¹⁻³ As a result, a charge dependence of nuclear forces of $\leq 2\%$ can be estimated.² Coulomb energy differences have also been calculated for excited states in $1p$ -shell mirror nuclei³ and satisfactory agreement is obtained if other effects such as the Thomas-Ehrman shift⁴ are taken into account. It would clearly be useful to know the results of similar calculations on other excited isobaric multiplets; however, very little experimental evidence exists for complete correspondences among excited states in isobaric multiplets of $T > \frac{1}{2}$.

The mass-14 triad is an especially attractive system to investigate since more is known about the $T=1$ levels of ^{14}N than of any other $T_z=0$ nucleus. In addition, the energy levels of ^{14}C have been extensively studied. All that is necessary to complete this triad is a knowledge of the levels of ^{14}O , which can be investigated through the $^{14}\text{N}(^3\text{He},t)^{14}\text{O}$ reaction. We have found

that the angular distributions observed in the $(^3\text{He},t)$ reaction on several light nuclei have characteristic shapes which depend on the nature of the single-particle transitions involved. By exploiting this effect in conjunction with other available data, it has been possible to assign most probable spins and parities to the levels observed in ^{14}O below 8 MeV. In this manner a correspondence has been established for six excited $T=1$ levels in all three members of the mass-14 triad.

II. EXPERIMENTAL

The $^{14}\text{N}(^3\text{He},t)^{14}\text{O}$ reaction was carried out at an energy of 44.6 MeV using a ^3He beam from the Berkeley 88-in. cyclotron. Particles were detected using a $(dE/dx-E)$ counter telescope which fed a particle identifier⁵; complete separation was obtained between tritons and deuterons. The (dE/dx) counter was a 300- μ phosphorus-diffused silicon detector while the E counter consisted of a 3-mm lithium-drifted silicon detector which was rotated 30° in order to stop the high-energy tritons. A more detailed discussion of the experimental equipment will be presented elsewhere.⁶

Both a N_2 gas target and a solid adenine ($\text{C}_5\text{H}_5\text{N}_5$) target were used. The gas was contained in a 7.66-cm diameter cell with a window of Havar⁷ foil 0.00025 cm thick. The solid target was made by evaporating ≈ 1.1 mg/cm² of adenine onto a 150 $\mu\text{g}/\text{cm}^2$ carbon backing. No detectable decomposition of the target was observed over a period of 48 h at beam intensities of 100–400 nA.

* Work performed under the auspices of the U. S. Atomic Energy Commission.

¹ B. C. Carlson and I. Talmi, *Phys. Rev.* **96**, 436 (1954); S. Sengupta, *Nucl. Phys.* **21**, 542 (1960); W. M. Fairbairn, *Proc. Phys. Soc. (London)* **77**, 599 (1961); L. Lovitch, *Nucl. Phys.* **46**, 353 (1963); **53**, 477 (1964); R. J. Blin-Stoyle and S. C. K. Nair, *Phys. Letters* **7**, 161 (1963); R. J. Blin-Stoyle, *Selected Topics in Nuclear Spectroscopy* (North-Holland Publishing Company, Amsterdam, 1964), p. 213; R. J. Blin-Stoyle and C. Yalgin, *Phys. Letters* **15**, 258 (1965).

² D. H. Wilkinson, *Phys. Rev. Letters* **13**, 571 (1964); D. H. Wilkinson and W. D. Hay, *Phys. Letters* **21**, 80 (1966).

³ W. M. Fairbairn, *Nucl. Phys.* **45**, 437 (1963).

⁴ R. G. Thomas, *Phys. Rev.* **81**, 148 (1951); **88**, 1109 (1952); J. B. Ehrman, *ibid.* **81**, 412 (1951).

⁵ F. S. Goulding, D. A. Landis, J. Cerny, and R. H. Pehl, *Nucl. Instr. Methods* **31**, 1 (1964).

⁶ D. G. Fleming, C. C. Maples, and J. Cerny (to be published).

⁷ Hamilton Watch Company, Waltham, Massachusetts.

Typical energy spectra are shown in Fig. 1; an energy resolution (full width at half-maximum) of 190 ± 10 keV was observed using the gas target while the adenine target gave a resolution of 155 ± 10 keV. This improvement in resolution was important in separating several levels in ^{14}O . The determination of the excitation energies of highly excited levels in ^{14}O was aided in the adenine-target measurements by the presence of the $^{12}\text{C}(^3\text{He},t)^{12}\text{N}$ ground-state transition which provided an internal calibration point at each angle; a mass excess of 17.349 MeV⁸ was used for ^{12}N .

The energy levels observed in the $^{14}\text{N}(^3\text{He},t)^{14}\text{O}$ reaction are summarized in Table I and compared with prior measurements⁹; spin and parity assignments are indicated and will be discussed below. The states at 5.91 ± 0.04 , 6.28 ± 0.03 and 6.60 ± 0.03 MeV are in good agreement with the levels observed by Towle and Macefield in the $^{12}\text{C}(^3\text{He},n)^{14}\text{O}$ reaction at 5.905 ± 0.012 ,

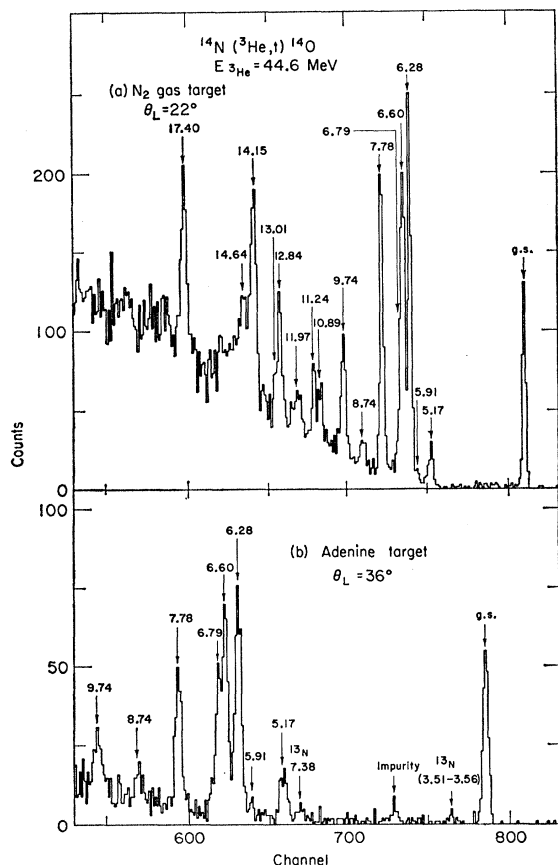


FIG. 1. Energy spectra for the $^{14}\text{N}(^3\text{He},t)^{14}\text{O}$ reaction at a ^3He energy of 44.6 MeV using (a) a N_2 gas target and (b) a solid adenine target.

⁸ R. W. Kavanagh, Phys. Rev. **133**, B1504 (1964).

⁹ T. Lauritsen and F. Ajzenberg-Selove, *Nuclear Data Sheets*, compiled by K. Way *et al.* (Printing and Publishing Office, National Academy of Sciences—National Research Council, Washington, D. C., 1962), sets 5 and 6.

TABLE I. Energy levels observed in ^{14}O .

$^{14}\text{N}(^3\text{He},t)^{14}\text{O}$ (Present work)		Values from Lauritsen <i>et al.</i> ^a	
Energy (MeV)	$J\pi$	Energy (MeV)	$J\pi$
0	0+	0	0+
5.17 ± 0.040	(1-)		
5.91 ± 0.040	(0+)	5.91 ± 0.012	
6.28 ± 0.030	(3-)	6.30 ± 0.030	
6.60 ± 0.030	2+	6.59 ± 0.012	
6.79 ± 0.030	(2-)		
7.78 ± 0.030	2+	~ 7.5	
8.74 ± 0.060			
9.74 ± 0.030		~ 9.3	
10.89 ± 0.050			
11.24 ± 0.050			
11.97	^b		
12.84 ± 0.050			
13.01 ± 0.050			
14.15 ± 0.040			
14.64 ± 0.060			
17.40 ± 0.060			

^a See Ref. 9.

^b Several levels are populated in this region.

6.30 ± 0.03 , and 6.586 ± 0.012 MeV, respectively.¹⁰ Angular distributions for the $^{14}\text{N}(^3\text{He},t)^{14}\text{O}$ reaction were obtained at laboratory angles between 12 and 60 deg and are presented in Fig. 2. The absolute cross sections are accurate to $\pm 10\%$. In all cases lines have been drawn through the experimental points to guide the eye.

III. RESULTS AND DISCUSSION

Before embarking on an analysis of the $^{14}\text{N}(^3\text{He},t)^{14}\text{O}$ reaction, we would like to summarize the experimental data concerning the $T=1$ levels of ^{14}N and ^{14}C . This information will also be referred to in Sec. IV where level shifts between the members of the $A=14$ triad are discussed.

A. The $T=1$ Levels in ^{14}N

The $T=1$ levels in ^{14}N below 11 MeV are quite well established; spin and parity assignments have been made and the dominant shell-model configurations of the states are known.^{9,11-13} The results are summarized in Table II.

B. The Energy Levels in ^{14}C

The energies of the low-lying levels in ^{14}C have been known for some time¹⁴ and are tabulated in Table III; however, the spin and parity assignments have not been definitely determined until quite recently. In 1960 Warburton and Pinkston¹¹ summarized the available

¹⁰ J. H. Towle and B. E. F. Macefield, Proc. Phys. Soc. (London) **77**, 399 (1961).

¹¹ E. K. Warburton and W. T. Pinkston, Phys. Rev. **118**, 733 (1960).

¹² H. J. Rose, Nucl. Phys. **19**, 113 (1960); H. J. Rose, F. Riess, and W. Trost, *ibid.* **52**, 481 (1964).

¹³ G. C. Ball and J. Cerny, Phys. Letters **21**, 551 (1966).

¹⁴ F. Ajzenberg-Selove and T. Lauritsen, Nucl. Phys. **11**, 1 (1959).

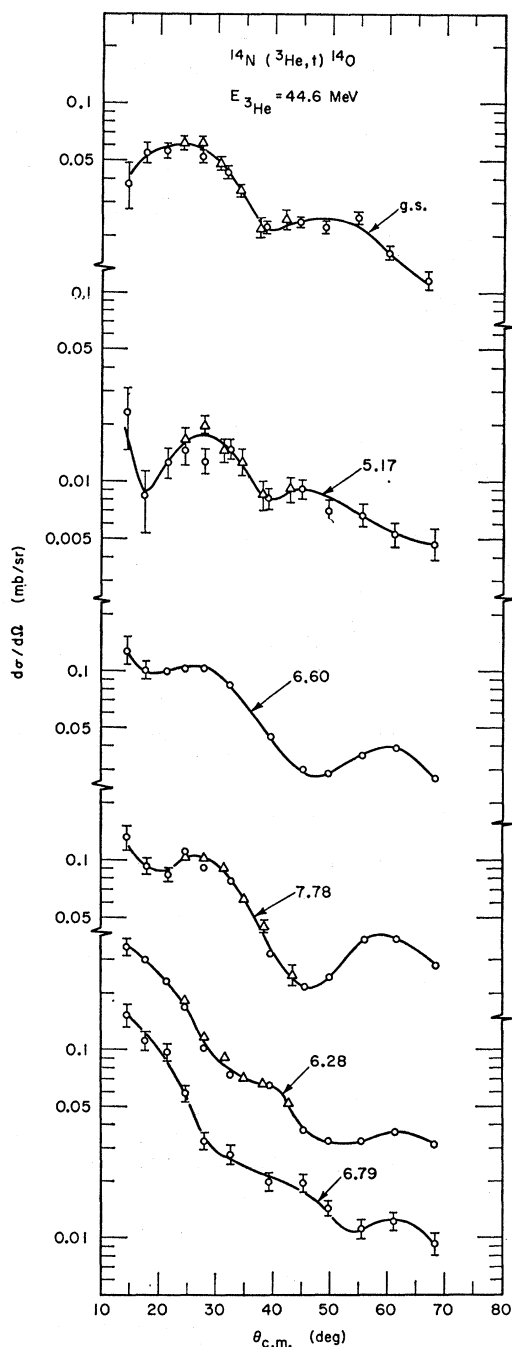


FIG. 2. Angular distributions from the $^{14}\text{N}(^3\text{He},t)^{14}\text{O}$ reaction. Points obtained from the gas target data are shown as triangles, while the solid adenine target data are indicated by circles. When no error bars are shown, the statistical error is contained within the point.

data on ^{14}C and ^{14}N and were able to assign every level below 9 MeV in ^{14}C to its analog in ^{14}N . More recent data have confirmed their assignments in every case.¹⁵⁻²¹

¹⁵ D. E. Alburger and E. K. Warburton, Phys. Rev. **132**, 790 (1963).

¹⁶ E. K. Warburton, D. E. Alburger, A. Gallmann, P. Wagner, and L. F. Chase, Jr., Phys. Rev. **133**, B42 (1964); D. E. Alburger,

Table III also summarizes the magnetic-pair-spectrometer measurements of electromagnetic transitions^{15,16} in ^{14}C and the experimental data on the $^{13}\text{C}(d,p\gamma)^{14}\text{C}$ reaction,^{17,18} which confirm the spin and/or parity assignments for several levels in ^{14}C . It can be seen from Table III that the only levels which cannot be definitely assigned from these experiments are those at 7.01 and 8.32 MeV. However, as previously suggested by Alburger and Warburton,¹⁵ there is strong indirect evidence that these levels both have spin and parity $2+$, since they are the only known levels of ^{14}C which could be the analogs of the 9.17- and 10.43-MeV levels in ^{14}N . The 7.01- and 8.32-MeV levels in ^{14}C are both strongly populated in the $^{12}\text{C}(t,p)^{14}\text{C}$ reaction^{19,20} and recent DWBA (distorted-wave Born approximation) analysis of these data²¹ also supports a $2+$ assignment for both levels (see Table III).

C. The $^{14}\text{N}(^3\text{He},t)^{14}\text{O}$ Reaction and Level Assignments in ^{14}O

An investigation of the $(^3\text{He},t)$ reaction in several light nuclei has been carried out. In particular, the $^{16}\text{O}(^3\text{He},t)^{16}\text{F}$ (see Ref. 22), $^{15}\text{N}(^3\text{He},t)^{15}\text{O}$, $^{14}\text{C}(^3\text{He},t)^{14}\text{N}$, and $^{14}\text{N}(^3\text{He},t)^{14}\text{O}$ reactions have been studied at 40.2, 39.8, 44.8, and 44.6 MeV, respectively. In general we have observed that many levels are populated in the $(^3\text{He},t)$ reaction and that the transition to the ground isobaric analog state does not dominate the spectrum. As might be expected, transitions which involve promotion of a single nucleon have relatively large cross sections, while those which involve promotion of two or more nucleons are generally much more weakly populated. The shapes and relative magnitudes of the

TABLE II. $T=1$ energy levels in ^{14}N .

Energy (MeV) ^a	$J\pi$	Dominant shell-model configuration ^b
2.31	0+	$(p_{1/2})^2$
8.06	1-	$(p_{1/2}, s_{1/2})$
8.62	0+	(s, d)
8.71	0-	$(p_{1/2}, s_{1/2})$
8.91	3-	$(p_{1/2}, d_{5/2})$
9.17	2+	$(s, d) + (p_{3/2}, p_{1/2})^{-1}$
9.51	2-	$(p_{1/2}, d_{5/2})$
10.43	2+	$(s, d) + (p_{3/2}, p_{1/2})^{-1}$
11.24	3-	
13.72 ± 0.04^c	$1+^c$	$(p_{3/2}, p_{1/2})^{-1^c}$

^a All energy levels without errors are known to ± 10 keV with the exception of the broad 8.71-MeV state (see Ref. 9).

^b Assignments made in Refs. 11 and 12.

^c See Ref. 13.

A. Gallmann, J. B. Nelson, J. T. Sample, and E. K. Warburton, *ibid.* **148**, 1050 (1966).

¹⁷ J. M. Lacambra, D. R. Tilley, N. R. Roberson, and R. M. Williamson, Nucl. Phys. **68**, 273 (1965).

¹⁸ F. Riess and W. Trost, Nucl. Phys. **78**, 385 (1966).

¹⁹ A. A. Jaffe, F. de S. Barros, P. D. Forsyth, J. Muto, I. J. Taylor, and S. Ramavataram, Proc. Phys. Soc. (London) **76**, 914 (1960).

²⁰ R. Middleton and D. J. Pullen, Nucl. Phys. **51**, 63 (1964).

²¹ R. N. Glover and A. D. W. Jones, Nucl. Phys. **81**, 277 (1966).

²² R. H. Pehl and J. Cerny, Phys. Letters **14**, 137 (1965).

TABLE III. Spin and parity assignments for low-lying levels in ^{14}C .

Energy ^a (MeV)	$J\pi$ "Best value"	Electromagnetic transitions in ^{14}C			$^{12}\text{C}(t,p)^{14}\text{C}$		
		Alburger and Warburton <i>et al.</i> ^b	$^{13}\text{C}(d,p\gamma)^{14}\text{C}$ Lacambra Riess <i>et al.</i> ^c <i>et al.</i> ^d	Ajzenberg- Selove <i>et al.</i> ^e	Plane-wave double- stripping theory Jaffe <i>et al.</i> ^f	Middleton <i>et al.</i> ^g	DWBA analysis Glover <i>et al.</i> ^h
0	0+			0+	0+	0+	0+
6.09	1-	1-	1-	1-	1-	(2+)	1-
6.58	0+	0+		(1-, 2±, 3-)	1-	1-	0+
6.72	3-	3-	3-	(3-, 2-)	(3-)	(2+)	3-
6.89	0-			0(-)	(weak)	(weak)	
7.01	(2+)				0+	(2+)	2+
7.34	2-	2-	2-	(2-, 3-)	(weak)	(weak)	
8.32	(2+)					2+	2+

^a All energy levels are known to ± 10 keV (see Refs. 9 and 14).

^b Angular-correlation measurements (see Ref. 17).

^c $J\pi$ assignments mainly from the $^{13}\text{C}(d,p)^{14}\text{C}$ reaction (see Ref. 14).

^d 11-MeV triton beam (see Ref. 20).

^e Magnetic pair spectrometer measurements (see Refs. 15 and 16).

^f γ polarization measurements (see Ref. 18).

^g 5.5-MeV triton beam (see Ref. 19).

^h DWBA analysis of data from Ref. 20 (see Ref. 21).

angular distributions arising from single-particle transitions appear to fall into groups which depend not only on the orbital angular momentum transfer but also on the specific shell-model transition involved. Such an effect is extremely useful in utilizing the $(^3\text{He}, t)$ reaction as a spectroscopic tool, as has already been indicated in the $^{16}\text{O}(^3\text{He}, t)^{16}\text{F}$ reaction.²² It is of interest that the inelastic scattering of α and ^3He particles^{23,24} in the $1p$ shell has also shown a similar effect. This appears to agree with recent theoretical formalisms²⁵ which treat the $(^3\text{He}, t)$ reaction as a change-exchange inelastic scattering process.

Several different single-particle transitions are expected in the $^{14}\text{N}(^3\text{He}, t)^{14}\text{O}$ reaction below an excitation of 9 MeV. In particular (compare Table II), $p_{3/2} \rightarrow p_{1/2}$, $p_{1/2} \rightarrow d_{5/2}$, and $p_{1/2} \rightarrow s_{1/2}$ transitions should be readily observed. As an aid in making spectroscopic assignments, the angular distributions from the $^{14}\text{N}(^3\text{He}, t)^{14}\text{O}$ reaction have been compared to similar, well-known single-particle transitions in the $^{15}\text{N}(^3\text{He}, t)^{15}\text{O}$ and $^{14}\text{C}(^3\text{He}, t)^{14}\text{N}$ reactions. A more complete report on the other reactions will be published later.²⁶

The level assignments will now be discussed individually according to the particular single-particle transition involved. Although the spin and parity assignments have been made primarily on the basis of the information obtained from the $(^3\text{He}, t)$ reaction, available data on the $^{16}\text{O}(p, t)^{16}\text{O}$ and $^{12}\text{C}(^3\text{He}, n)^{14}\text{O}$ reactions^{27,10} were also utilized.

The 6.60- and 7.78-MeV Levels in ^{14}O

It has been shown that the 9.17- and 10.43-MeV levels in ^{14}N contain approximately equal amplitudes of $(p_{3/2}, p_{1/2})^{-1}$ and (s, d) configurations.^{12,13} The identification of the analogs to these levels in ^{14}O should be greatly simplified in the $^{14}\text{N}(^3\text{He}, t)^{14}\text{O}$ reaction since it will primarily be sensitive to the $(p_{3/2}, p_{1/2})^{-1}$ part of the wave function, and so both levels in ^{14}O should have angular distributions which are similar in shape and approximately equal in magnitude. In Fig. 2 it can be seen that the transitions to the 6.60- and 7.78-MeV levels in ^{14}O have (1) nearly equal magnitudes and (2) almost identical and quite distinct angular distributions (compared with transitions to all other levels in ^{14}O below 9 MeV).

The angular distributions for these two levels are compared in Fig. 3 with known $(^3\text{He}, t)$, $p_{3/2} \rightarrow p_{1/2}$ transitions to the $\frac{3}{2}^-$ level in ^{15}O at 6.18 MeV²⁸ and to the $1+$ level in ^{14}N at 3.95 MeV. All four distributions show predominantly a similar shape when plotted as a function of the linear momentum transfer $(k_i - k_f)$; the radius of interaction (R) will be assumed to be approximately constant for all transitions in mass 14 and 15. A $p_{3/2} \rightarrow p_{1/2}$ transition can involve an orbital angular momentum transfer of $l=0$ or 2. Experimentally we have observed that transitions which must be $l=0$ (the 2.31-MeV level in ^{14}N) or $l=2$ (the 7.03-MeV level in ^{14}N) have quite different angular distributions.²⁶ For all transitions compared in Fig. 3, however, both l values are allowed and the shapes of the angular distributions, although similar, indicate that both l transfers are involved. In particular, the $1+$ level in

²³ B. G. Harvey, J. R. Meriwether, J. Mahoney, A. Bussièrè de Nercy, and D. J. Horen, Phys. Rev. **146**, 712 (1966).

²⁴ The inelastic ^3He scattering data were obtained in conjunction with these $(^3\text{He}, t)$ experiments.

²⁵ R. M. Drisko, R. H. Bassel, and G. R. Satchler, Phys. Letters **2**, 318 (1962); V. A. Madsen, Nucl. Phys. **80**, 177 (1966); G. R. Satchler, *ibid.* **77**, 481 (1966).

²⁶ G. C. Ball and J. Cerny (unpublished data).

²⁷ J. Cerny and R. H. Pehl, Argonne National Laboratory Report No. ANL-6848, 1964 (unpublished), p. 208.

²⁸ In the $^{15}\text{N}(^3\text{He}, t)^{15}\text{O}$ reaction a large transition to the 6.18-MeV level was observed, with a very small population of the $\frac{3}{2}^-$ level at 8.98-MeV. This is in good agreement with recent information obtained from the $^{16}\text{O}(^3\text{He}, \alpha)^{16}\text{O}$ [E. K. Warburton, P. D. Parker, and P. F. Donovan, Phys. Letters **19**, 397 (1965)] and $^{16}\text{O}(p, d)^{16}\text{O}$ [C. R. Gruhn and E. Kashy, Bull. Am. Phys. Soc. **11**, 471 (1966)] reactions which confirmed that the 6.18-MeV level contains most of the $p_{3/2}^{-1}$ strength.

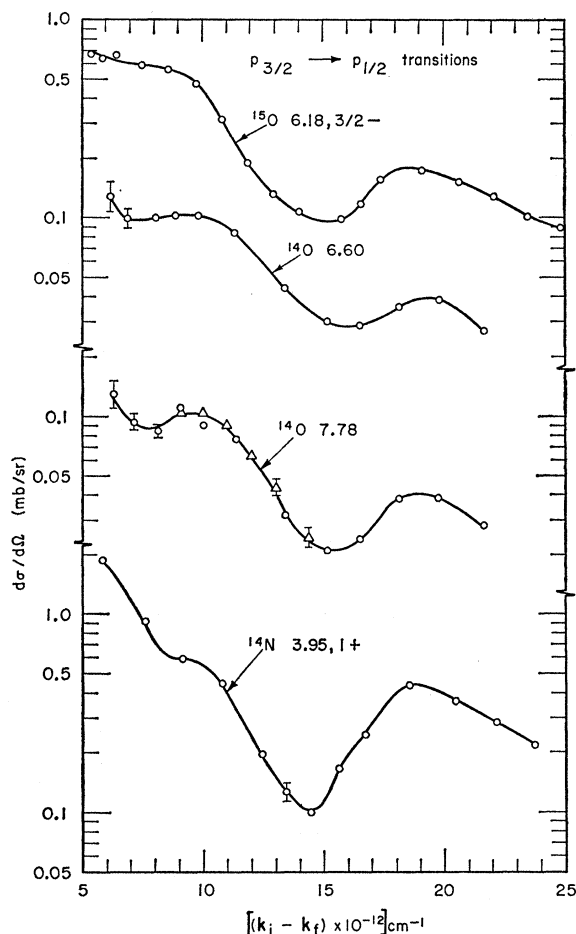


FIG. 3. Angular distributions for $p_{3/2} \rightarrow p_{1/2}$ transitions observed in the $^{15}\text{N}(^3\text{He},t)^{15}\text{O}$, $^{14}\text{C}(^3\text{He},t)^{14}\text{N}$, and $^{14}\text{N}(^3\text{He},t)^{14}\text{O}$ reactions. All absolute cross sections are accurate to $\pm 10\%$ with the exception of the $^{14}\text{C}(^3\text{He},t)^{14}\text{N}$ reaction where the absolute cross sections are accurate to $\pm 25\%$ due to an uncertainty in the ^{14}C target thickness.

^{14}N appears to have relatively more $l=2$ character at forward angles.

Evidence from the $^{16}\text{O}(p,t)^{14}\text{O}$ reaction²⁷ confirms a $2+$ assignment for both the 6.60- and 7.78-MeV levels in ^{14}O . The two-neutron pick-up data show that these levels²⁹ are the only excited states which are strongly (and nearly equally)³⁰ populated below 9 MeV and that their angular distributions have an $L=2$ character. This reaction should preferentially populate the analogs to the 9.17- and 10.43-MeV levels in ^{14}N , since they will be the only p^{-2} excited states in ^{14}O below 9 MeV (see Table II).

²⁹ In Ref. 27, the analogs to the 9.17- and 10.43-MeV levels in ^{14}N were reported to have excitation energies in ^{14}O of 6.3 and 7.5 MeV, respectively, assuming that the 7.5-MeV level was known. These data have been reanalyzed using an energy scale based only on the ^{14}O ground state; good agreement with the present values was obtained.

³⁰ The $^{16}\text{O}(p,t)^{14}\text{O}$ reaction has recently been repeated with much better energy resolution at a proton energy of 54 MeV. D. G. Fleming and J. Cerny (unpublished data).

The 6.28- and 6.79-MeV Levels in ^{14}O

Among the states which are populated fairly strongly in the $^{14}\text{N}(^3\text{He},t)^{14}\text{O}$ reaction are those at 6.28 and 6.79 MeV. The angular distributions to these states are similar, being strongly forward peaked at small angles and appearing to have a weak second maximum at $\theta_{\text{c.m.}} = 35\text{--}40$ deg and a minimum at $\theta_{\text{c.m.}} = 50\text{--}55$ deg (see Fig. 2). This shape is characteristic of several known $p_{1/2} \rightarrow d_{5/2}$ transitions observed in the $^{14}\text{C}(^3\text{He},t)^{14}\text{N}$ and $^{15}\text{N}(^3\text{He},t)^{15}\text{O}$ reactions; a number of these transitions are compared in Fig. 4. The angular distributions for the $3-$ and $2-$, $T=1$ levels in ^{14}N at 8.91 and 9.51 MeV, respectively, are not presented since these states could not be resolved from neighboring $T=0$ and $T=1$ levels. A $p_{1/2} \rightarrow d_{5/2}$ transition can involve an orbital angular momentum transfer of $l=1$ or 3. In Fig. 4, two transitions (the ^{15}O , 7.28-MeV and ^{14}N , 5.83-MeV levels) must be $l=3$; however, the general similarity of the six transitions appears to

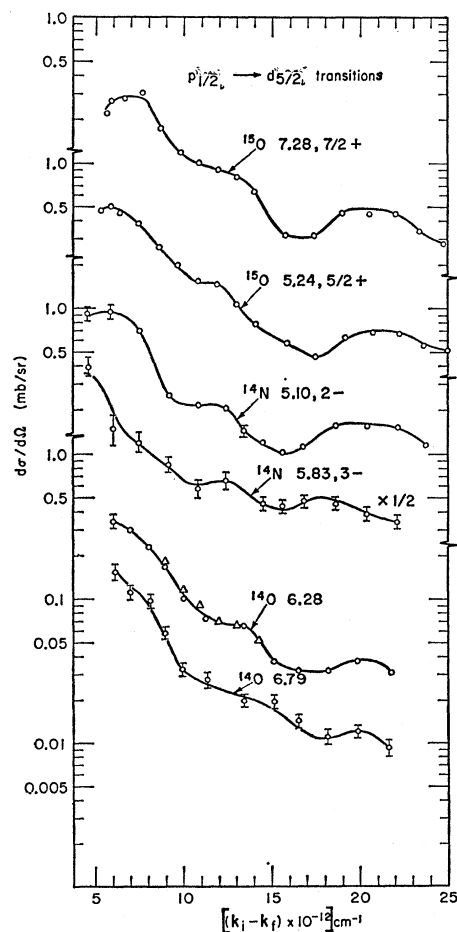


FIG. 4. Angular distributions for $p_{1/2} \rightarrow d_{5/2}$ transitions observed in the $^{15}\text{N}(^3\text{He},t)^{15}\text{O}$, $^{14}\text{C}(^3\text{He},t)^{14}\text{N}$, and $^{14}\text{N}(^3\text{He},t)^{14}\text{O}$ reactions. The contribution to the ^{15}N , 5.24-MeV level from the unresolved $\frac{3}{2}+$ state at 5.19 MeV is assumed to be small.

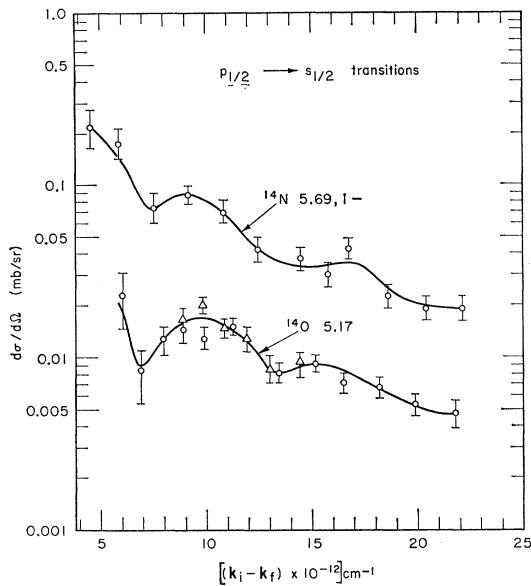


FIG. 5. Angular distributions for $p_{1/2} \rightarrow s_{1/2}$ transitions observed in the $^{14}\text{C}(\text{}^3\text{He},t)^{14}\text{N}$ and $^{14}\text{N}(\text{}^3\text{He},t)^{14}\text{O}$ reactions.

indicate that they all prefer a somewhat dominant $l=3$ transfer.

From this evidence one would consider the 6.28- and 6.79-MeV levels in ^{14}O to clearly be of $(p_{1/2}, d_{5/2})$ character. The consistent pattern found in the $T=1$ level shifts (see Sec. IV) leads us to consider these to be the analogs of the $(p_{1/2}, d_{5/2})_{3-, T=1}$ and $(p_{1/2}, d_{5/2})_{2-, T=1}$ levels in ^{14}N at 8.91 and 9.51 MeV, respectively.

The 5.17- and 5.91-MeV Levels in ^{14}O

There are only three $T=1$ levels in ^{14}N below 11 MeV which have not so far been assigned an analog in ^{14}O . The analog to the ^{14}N , 8.62-MeV level should be weakly populated in the $(\text{}^3\text{He},t)$ reaction, since it has the configuration $(s, d)_{0+, T=1}$. The other two levels in ^{14}N lie at 8.06- and 8.71-MeV excitation and arise from a $(p_{1/2}, s_{1/2})$ configuration; therefore, the ^{14}O analogs to these levels will be populated by a $p_{1/2} \rightarrow s_{1/2}$ transition. Under our experimental conditions, this type of promotion, which could only be an $l=1$ transition, has been found to possess a much smaller cross section than the other allowed single-particle transitions to low-lying orbitals: small relative cross sections are observed both in the $^{16}\text{O}(\text{}^3\text{He},t)^{16}\text{F}$ reaction²² in transitions to the ground, $0-$ and 0.200 MeV, $1-$ levels of ^{16}F and in the $^{14}\text{C}(\text{}^3\text{He},t)^{14}\text{N}$ reaction in transitions to the 4.91 MeV, $0-$ and 5.69 MeV, $1-$ levels of ^{14}N . The 8.71 MeV, $0-$ level in ^{14}N is unbound by 1.16 MeV and has a width of $\cong 500$ keV.⁹ Neglecting level shifts, the ^{14}O analog to this state should occur near 6.4 MeV; since ^{14}O is unbound at 4.626 MeV, the $0-$ level in ^{14}O might be expected to have a comparable or greater width

making it difficult to observe, especially since $p_{1/2} \rightarrow s_{1/2}$ transitions are weakly populated.

Two weakly populated states at 5.17 and 5.91 MeV are the only levels observed in the $^{14}\text{N}(\text{}^3\text{He},t)^{14}\text{O}$ reaction below 8 MeV which have not been assigned. On the basis of its excitation energy, the 5.17-MeV level is the only known state which could be the analog to the 8.06 MeV, $1-$ level in ^{14}N (see Sec. IV). The angular distribution for this state has a $p_{1/2} \rightarrow s_{1/2}$ character and is compared in Fig. 5 with the known transition to the $(p_{1/2}, s_{1/2})_{1-, T=0}$ level in ^{14}N at 5.69 MeV. [Angular distributions for other $p_{1/2} \rightarrow s_{1/2}$ transitions in the $^{14}\text{C}(\text{}^3\text{He},t)^{14}\text{N}$ reaction could not be obtained. The 8.71-MeV level was too broad to be observed, the 8.06-MeV level could not be separated from the 7.97-MeV level and the 4.91-MeV level was only observed at a few angles.] The 5.91-MeV level in ^{14}O has a width of $\lesssim 60$ keV¹⁰ and is weakly populated in the $^{14}\text{N}(\text{}^3\text{He},t)^{14}\text{O}$ reaction. Since it is a sharp state, this level could only be the analog of the $(s, d)_{0+, T=1}$ state in ^{14}N at 8.62 MeV.

The Levels in ^{14}O above 8 MeV

Little can be said at present concerning the other levels in ^{14}O which are observed in the $^{14}\text{N}(\text{}^3\text{He},t)^{14}\text{O}$ reaction. Several of the levels which are strongly populated above 8 MeV probably arise from other single-particle transitions, such as $p_{1/2} \rightarrow d_{3/2}$ or $p_{3/2} \rightarrow d_{5/2}$ transitions. Of additional interest would be the ^{14}O analog to the 13.72 MeV, $(p_{3/2}, p_{1/2})_{-1+, T=1}$ level in ^{14}N ,

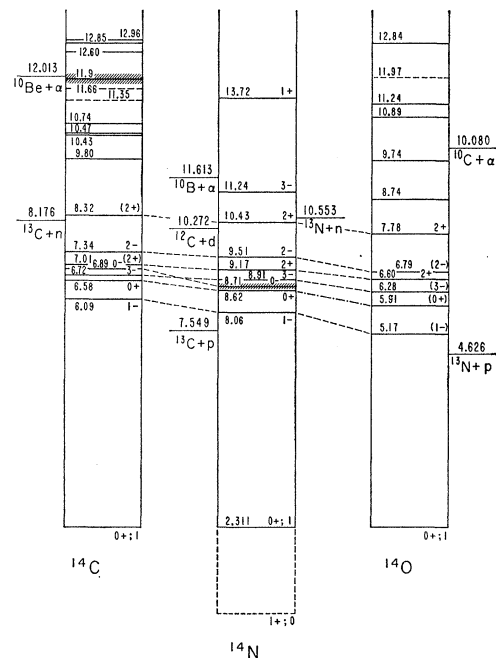


FIG. 6. Energy-level diagram for the $T=1$ levels in ^{14}C , ^{14}N , and ^{14}O . Uncertain $J\pi$ assignments are enclosed in parentheses. The levels are connected by a dashed line if the correspondence is considered well established and by a dot-dash line if the correspondence is considered tentative.

TABLE IV. $T=1$ levels in the mass-14 triad.

^{14}C Energy (MeV)	Level shift (keV) ^a	^{14}N Energy (MeV)	$J\pi$	Dominant shell-model configuration	Level shift (keV) ^a	^{14}O Energy (MeV)
0	...	2.31	0+	$(p_{1/2})^2$...	0
6.09	340	8.06	1-	$(p_{1/2}, s_{1/2})$	580	5.17
6.58	270	8.62	0+	(s, d)	400	5.91
6.89	490	8.71	0-	$(p_{1/2}, s_{1/2})$		
6.72	120	8.91	3-	$(p_{1/2}, d_{5/2})$	320	6.28
7.01	150	9.17	2+	$(sd) + (p_{3/2}, p_{1/2})^{-1}$	260	6.60
7.34	140	9.51	2-	$(p_{1/2}, d_{5/2})$	410	6.79
8.32	200	10.43	2+	$(sd) + (p_{3/2}, p_{1/2})^{-1}$	340	7.78

^a The level shifts are calculated relative to the ground-state multiplet.

which does not appear to be strongly populated in the $^{14}\text{N}({}^3\text{He}, t){}^{14}\text{O}$ reaction.

IV. A COMPARISON OF $T=1$ LEVELS IN THE MASS-14 TRIAD

An energy-level diagram shown in Fig. 6 summarizes the available information on the $T=1$ levels of ^{14}C , ^{14}N , and ^{14}O . Level shifts for the completed excited multiplets, relative to the ground isobaric multiplet, are presented in Table IV. From this table it can be seen that all levels in ^{14}N are shifted downward relative to their position in ^{14}C , with the 0- and 1- levels undergoing a stronger shift. Since all levels in ^{14}C below 8.176 MeV are bound, whereas all but the lowest $T=1$ level in ^{14}N (and ^{14}O) are unbound (see Fig. 6), a major component of these strong shifts, in addition to the Coulomb displacement, is certainly the Thomas-Ehrman effect which would be most pronounced for an s -state proton. A similar general shift is observed for all levels in ^{14}O relative to their positions in ^{14}N , with the 5.17 MeV, 1- level the most strongly shifted, as expected. The consistent pattern of the level shifts from ^{14}C to ^{14}N to ^{14}O would be drastically altered if any of the

levels in ^{14}O were incorrectly assigned. For example, if the 3- and 2- levels at 6.28 and 6.79 MeV were in fact 2- and 3-, respectively, then the 3- level would be shifted *upward* 190 keV while the 2- level was shifted downward by 920 keV.

Tombrello³¹ has recently proposed a simple two-body model for relating levels within an isobaric multiplet. This model assumes that the level has the configuration of a single nucleon outside an $A-1$ core, where the nucleon and the core interact through an attractive nuclear potential of a Woods-Saxon form. If the nucleon is a proton, then a repulsive potential due to the Coulomb field is also introduced. This model was able to account for both the Coulomb energy difference and the Thomas-Ehrman shift observed for several well-known cases in $T=\frac{1}{2}$ nuclei and was successfully applied in interpreting excited $T=1$ states in the $A=8$ and $A=16$ nuclei.³¹ Tombrello has made available to us³² the results of a similar calculation for the 0-, 1-, 2-, and 3- levels in ^{14}C , ^{14}N , and ^{14}O ; these results are shown in Table V. The V_0 's represent the depth of the potential well required to reproduce the known positions of the levels in each nucleus. Good agreement with our assignments is obtained if one notes the trend observed by Tombrello³¹ that the V_0 for the neutron configuration was always slightly greater than the V_0 for the proton configuration. These calculations also imply that the V_0 for the 0- level in ^{14}O should be $\cong 45.3$ MeV corresponding to an excitation energy of 5.76 MeV.

TABLE V. Values of V_0 (MeV) for $T=1$ levels in ^{14}C , ^{14}N , and ^{14}O for configurations based on a nucleon plus an $A=13$ core.^a

$J\pi$	^{14}C ($^{13}\text{C}+n$)	^{14}N ($^{13}\text{N}+n$)	^{14}N ($^{13}\text{C}+p$)	Average	^{14}O ($^{13}\text{N}+p$)
1-	48.07	49.16	46.47	47.82	47.65
0-	45.70	47.37	43.67	45.52 ^b	...
3-	46.75	47.11	46.05	46.58	46.35
2-	45.48	45.89	44.63	45.26	45.08

^a The Woods-Saxon potential had a nuclear radius $R=3.33F$ and a surface diffuseness $a=0.5F$.

^b These calculations arise from an energy of 8.71 MeV for the 0-, $T=1$ state in ^{14}N . When the more recent measurement of 8.82 ± 0.05 MeV [V. A. Latorre and J. C. Armstrong, Phys. Rev. **144**, 891 (1966)] for this level was used, an average potential of 45.17 MeV was obtained.

ACKNOWLEDGMENTS

We would like to thank Joanne Sauer, of the University of Washington, for suggesting the adenine target and also Claude Ellsworth for preparing it.

³¹ T. A. Tombrello, Phys. Letters **23**, 134 (1966).

³² T. A. Tombrello (private communication).